

Project work

Simon Margido Urdahl

Influencing fish migration by creating and altering vortices in turbulent flow

Trondheim, 12 2021

NTNU
Norwegian University of
Science and Technology
Faculty of Engineering
Department of Energy and Process Engineering



NTNU – Trondheim
Norwegian University of
Science and Technology

PROJECT WORK

for
Simon Urdahl
Autumn 2021

FishPath

Background

Safe passage of downstream migrating fish is a challenge for the hydropower industry. The number of fish entering the intake to existing hydropower plants is often too high and fish mortality should be reduced. Currently available solutions depend on retrofitting of large fined meshed rack- and bypass constructions. In this project, alternative solutions are investigated based on behavioral guiding of fish.

Research on alternative behavioral guiding systems is currently rather limited, focusing on guiding racks or repulsion systems. However, recent advances in the knowledge on behavioral responses to turbulence eddies point toward the possibility of exploiting the species innate attraction and repulsion for eddies of different characteristics to create migration paths passed the intakes. It has been shown that some eddies may boost swimming whereas others can hamper swimming. Turbulence eddies may be crated in new rack designs or alternative structures that efficiently interconnects the desired turbulence eddies into a migration path. Such constructions are expected to be less demanding both technologically and in terms of cost.

The FishPath-project is a project funded by the Norwegian Research Council and the student will be a part of the project team.

Objective

To explore the possibility of using inter-connected turbulence eddies as paths for fish downstream migration passed hydropower intakes

The following tasks are to be considered:

1. Literature study
 - a. Turbulent eddies/ vortices
 - b. Vortex generators
2. Software knowledge
 - a. Matlab will be used for the evaluation of the measurements
3. Preparations in the Waterpower Laboratory
 - a. Make drawings for the measurement setup of the flume in the Waterpower Laboratory in collaboration with supervisors
4. If the Waterpower Laboratory is in operation and time allows it, the following can be carried out:
 - a. Learn how to use the PIV-measurement system
 - b. Installation of a vortex generator and carry out PIV-measurements
 - c. Learn how to use CAD-drawing by CREO
 - d. Develop procedures for calibration of PIV

-- “ --

The project work comprises 15 ECTS credits.

The work shall be edited as a scientific report, including a table of contents, a summary in Norwegian, conclusion, an index of literature etc. When writing the report, the candidate must emphasise a clearly arranged and well-written text. To facilitate the reading of the report, it is important that references for corresponding text, tables and figures are clearly stated both places.

By the evaluation of the work the following will be greatly emphasised: The results should be thoroughly treated, presented in clearly arranged tables and/or graphics and discussed in detail.

The candidate is responsible for keeping contact with the subject teacher and teaching supervisors.

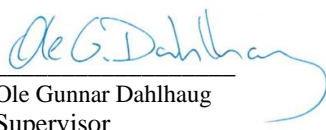
Risk assessment of the candidate's work shall be carried out according to the department's procedures. The risk assessment must be documented and included as part of the final report. Events related to the candidate's work adversely affecting the health, safety or security, must be documented and included as part of the final report. If the documentation on risk assessment represents a large number of pages, the full version is to be submitted electronically to the supervisor and an excerpt is included in the report.

According to "Utfyllende regler til studieforskriften for teknologistudiet/sivilingeniørstudiet ved NTNU" § 20, the Department of Energy and Process Engineering reserves all rights to use the results and data for lectures, research and future publications.

Submission deadline: 16th December 2021

- Work to be done in the Waterpower Laboratory
 Field work

Department for Energy and Process Engineering, *August 2021*


Ole Gunnar Dahlhaug
Supervisor

Co-Supervisor(s): Bjørn Winther Solemslie (Bjorn.Solemslie@nina.no)
Kristian Sagmo (Kristian.Sagmo@ntnu.no)



Abstract

Currently, the amount of fish entering hydropower plant intakes is often excessive, and fish mortality should be reduced. One method that will be investigated by a project called FishPath is to direct the fish away from the intakes using vortices and turbulence. This thesis aims to contribute to the research by looking into the literature on how to construct and adjust vortex parameters, in order to make future experiments on fish easier.

The wake behind cylinders with circular, triangular and square cross-sections as well as wing tips and the half delta vortex generator have been studied. Methods to create a stable flow regime, and modify parameters such as circulation, frequency of shedding, streamwise velocity, size and orientation have been reviewed in literature. The results show a varying degree of precision. There is a great amount of literature on a circular cylinder, which leads to good empirical relations, but little research has been conducted for cylinders with triangular and square cylinders. For the wing tip and the half delta vortex generator, a vast amount of literature on aerodynamic performance exist, but not so much on the vortices themselves. Nonetheless, for each shape and vortex parameter, some relationships with differing degrees of precision have been discovered.

A design concept for an experimental rig has been created to enable the evaluation of the findings experimentally in the future. The design was created to ensure good flow conditions and the usage of Particle Velocimetry Imaging. If a good description of how to make and change vortices can be found and validated, real-world tests on fish will be easier to conduct, allowing researchers to learn more about which parameters affect fish and in what ways.



Sammendrag

I dag er antall fisk som havner i inntaket på vannkraftverk ofte for høyt, og fiskedødeligheten bør reduseres. En metode som vil bli undersøkt av prosjektet FishPath er å lede fisken bort fra inntaket ved hjelp av virvler og turbulens. Dette prosjektet ønsker å bidra til prosjektet ved å undersøke litteratur om hvordan man kan opprette og endre virvelparametere, slik at eksperimenter på fisk i fremtiden vil være enklere.

Kjølvannet bak sylindere med sirkulære, trekantede og firkantede tverrsnitt samt vingespisser og virvelgeneratorer i halv-deltaform er studert. Metoder til skape et stabilt strømningsregime, og modifisere parametere som sirkulasjon, frekvens av virvelavgivelser, strømningshastighet bak formene, størrelse og orientering er gjennomgått i litteraturen. Resultatene viser varierende grad av presisjon. Det finnes en enorm mengde litteratur på en sirkulær sylinder, noe som resulterer i gode empiriske relasjoner, men det finnes mindre for sylindere med trekantede og firkantede tverrsnitt. For vingespissen og virvelgeneratoren finnes det en stor mengde litteratur om aerodynamisk ytelse, men ikke så mye om selve virvlene. Likevel er relasjoner av varierende grad av presisjon funnet for hver form og virvelparameter.

Noen av funnene vil bli testet eksperimentelt i fremtiden, så et designforslag av forsøksriggen er laget. Designet er laget for å sikre gode strømningsforhold og sikre muligheten til å kunne bruke Partikkelbilde-hastighetsmåling (PIV). Hvis en god beskrivelse blir funnet og validert om hvordan man oppretter og modifiserer virvler, vil forsøkene på ekte fisk lettere kunne øke vår forståelse på hvilke parametere som påvirker fisk og på hvilken måte.

Contents

Abstract	5
Sammendrag	7
Contents	9
List of tables	11
List of figures	14
Nomenclature	15
1 Introduction	1
2 Vortex tuning - Previous works	3
2.1 Fluid flow theory	3
2.2 Litterature review	8
3 Preperation for experiment	21
3.1 Previous works - experimental procedure	21
3.2 Design and preperations for experiment	25

10	10
<hr/>	
4 Results and discussions	29
4.1 Vortex tuning	29
4.2 Experimental test section	32
5 Conclusions	35
6 Future work	37
References	39
A Appendix A	43

List of Tables

2.1	Parameters for an eddy and a fish, and how to calculate them. Formulas from [1]	10
2.2	Flow regimes behind a circular cylinder [2]	11
2.3	Wake characteristics of sub critical flow for non circular objects	15
2.4	Wake characteristics of critical and super critical flow for non circular objects	15
3.1	Design consideration for designing the experimental rig at VKL.	28
4.1	Vortex tuning for a delta half wing vortex generator	29
4.2	Vortex tuning for a Von Karman street	30
4.3	Vortex tuning for a wing tip	31
4.4	Experimental rig parameters for the suggested design.	34

List of Figures

2.1	A typical Von Karman vortex street [3]	6
2.2	Wake	6
2.3	Lifting line structure [4]	7
2.4	Pitch, yaw and roll on a fish [5]	9
2.5	A fish exploiting energy in a Von Karman vortex street [6]	9
2.6	Streamwise turbulent intensity [7], where case A, B and C are numerical results. Case A is a smooth cylinder, while case B and C are two versions of grooved cylinders.	12
2.7	St vs Re for a circular cylinder. The figure is plotted by Techet for MIT OSW [8] with data from Lienhard [9], Roshko [10] and Achenbach Heinecke [11]	12
2.8	Dimensionalized streamwise velocity from experiments behind a circular cylinder [7].	13
2.9	Overview of how the Strouhal number varies for different Re for a selection of bluff bodies [2]	14
2.10	The shape of the cross sections that will be studied [12]	14
2.11	Shed circulation of an elliptical loaded wing. $\Gamma_0 = 500m^2/s, b = 60m$ [13]	16
2.12	Half delta wing vortex generator [14]	18

2.13	Trailing vortices of a delta wing [15]	19
2.14	The sweep angle [16]. Photo to the left by Bill Abbott	19
3.1	Experimental rig in the water channel. Drawing by Bjørn Winther Solemslie.	22
3.2	Illustration of a PIV set-up [17]	22
3.3	Relations between focal length, working distance and field of view [18]	23
3.4	The angle of incidence equals the angle of reflection [19]	23
3.5	The concept of performing PIV in a non-transparent water channel.	26
3.6	Flows that will be considered captured by PIV. The side walls are solids that can not be seen through.	27
4.1	Design proposal for the water channel, birds eye view.	33
4.2	Design proposal for the water channel, sideways view	33

Nomenclature

Abbreviation

BL	Boundary layer
CFD	Computational Fluid Dynamics
FOV	Field of Interest
LE	Leading edge
NTNU	Norwegian University of Science and Technology
PIV	Particle Image Velocimetry
VKL	Waterpower Laboratory

Latin symbols

A	Area (m^2)
b	Spanwise half-length of wing (m)
D	Diameter (m)
d	depth (m)
f	Frequency (Hz)
F'	Sectional force (N)
g	Gravitational acceleration ($m\ s^{-2}$)
h	Distance perpendicular to vortex filament ($m\ s^{-1}$)

I	Linear impulse (N s)
i	Angle of incidence ($^{\circ}$)
\mathbf{l}	Vector element of integration part (m)
L	Length in streamwise direction (m)
l	Lateral length (m)
P	Wetted perimeter (m)
r	Angle of reflection ($^{\circ}$)
S	Area of wing (m^2)
T	Thrust (N)
\mathbf{u}	Dataset of values of streamwise velocities ($m\ s^{-1}$)
U	Mean streamwise velocity ($m\ s^{-1}$)
u	Streamwise velocity ($m\ s^{-1}$)
u'	Fluctuation streamwise velocity ($m\ s^{-1}$)
u^*	Friction velocity ($m\ s^{-1}$)
\mathbf{V}	Velocity field ($m\ s^{-1}$)
v	Lateral velocity ($m\ s^{-1}$)
w	Spanwise velocity ($m\ s^{-1}$)

Dimensionless numbers

AR	Aspect Ratio
C	Contraction ratio
Fr	Froude number
Re	Reynolds number
St	Strouhal number
TI	Turbulent intensity

Greek symbols

β	Swirl angle ($^{\circ}$)
ϵ	Equivalent sand-grain roughness (m)
Γ	Circulation ($m^2 s^{-1}$)
ω	Angular velocity ($rad s^{-1}$)
ρ	Density ($kg m^{-3}$)
τ	Shear stress ($N m^{-2}$)
θ	Yaw angle ($^{\circ}$)
ν	Kinematic viscosity ($m^2 s^{-1}$)
ζ	Vorticity ($m s^{-2}$)

Superscripts and subscripts

c	Characteristic
conv	Converging
e	eddy
f	fish
h	Hydraulic
L	Lift
m	Mean
r	Rotational
s	Deficit
t	Tangential
w	Wall
∞	Free stream

Chapter 1

Introduction

The number of fish entering the intakes of hydropower plants is currently too high, and the fish mortality rate should be reduced. There are solutions to this problem, such as building solid bypass structures or fine-meshed grids. However, because this can be costly to construct in a large flowing river, the FishPath project aims to investigate fish behavioral guiding systems employing turbulence and vortices. The Norwegian Institute for Nature Research (NINA) is leading FishPath, although it has several partners in research and industry. The Waterpower Laboratory (VKL) at the Norwegian University of Science and Technology (NTNU), for whom this project thesis was written, is one of the partners. The responsibility of VKL in the project is to create various forms of flows that may then be utilized to investigate if the various types of flows will attract, repel, or do nothing for the routes of various types of fish.

The purpose of this project is to investigate in literature what kind of vortices that can be produced in a river and how to modify the parameters of the vortices. The project will also prepare for a measurement set up in the water flume at VKL in preparation for testing the literature experimentally. The experiments will be conducted for the continuation of this project as the master thesis next academic semester. For the FishPath project, it will most likely be a grid of several vortex generators, but the scope of this work will only investigate vortices created by single objects. The ultimate goal for the project and master thesis is to contribute to a catalogue of vortices NINA can choose from, based on literature as well as experiments.

Chapter 2

Vortex tuning - Previous works

This chapter covers theory for fluid dynamics followed by a literature review on vortex tuning.

2.1 Fluid flow theory

This section will present the basic theory behind vortices, turbulence, wakes, aerodynamics and other flow characteristics which is needed to understand the topics that will be addressed in the literature review.

2.1.1 Turbulence

A flow can either be turbulent, laminar or transitional. Turbulent flow is characterized as chaotic and the velocity field is random. It can be difficult to predict and describe the flow. The motion of every single droplet or eddy is unpredictable, but statistical analyzes can be used to describe the constraints of the randomness in the velocity field, \mathbf{V} . The variance, standard deviation and mean for the velocity field can be found, and each velocity value, e.g the streamwise velocity u , can be split into a mean value, U , and the fluctuation, u' as shown in Equation 2.1 [20].

$$u \equiv U + u'. \quad (2.1)$$

One way to measure the magnitude of the turbulence is by the turbulence intensity, TI, which is defined as root mean square turbulence divided by the freestream velocity [2] shown in Equation 2.2,

$$TI = \frac{\sqrt{\mathbf{u}'^2}}{U} \quad (2.2)$$

where \mathbf{u} is a dataset of values of streamwise velocities for a specific location at a time period. A TI of 10% is considered high. Reynolds number (Re) is a non dimensional number which is closely linked to turbulence and is defined in Equation 2.3 [21]. It is the ratio of the momentum to kinematic viscosity.

$$Re = \frac{uL_c}{\nu}, \quad (2.3)$$

where L_c is the characteristic length in the streamwise direction and ν is the kinematic viscosity. The characteristic length for a circle is the diameter (D). When the Reynolds number is sufficiently big, the flow will become turbulent. This is due to the fact that the large scales of motion will not be damped by viscosity because the momentum forces is much bigger than the viscosity. Instead, the energy of the big movements of the characteristic speed and length will be transferred to smaller and smaller scales by inviscid processes. This keeps on going until the movements are so small that viscosity can damp the movement, and dissipate the energy to heat. This is a characteristic of turbulent flow; A combination of movements of many different scales. [20].

2.1.2 Vortex

The inclusion of vortices is important during the analysis of a flow, as they are often a fundamental part of the dynamics and structure. Cengel and Cimbala [21] defines a vortex as a local structure in a fluid flow characterized by a concentration of vorticity in a tubular core with circular streamlines around the core axis. Vorticity (ζ) is a measurement of the rotation of a fluid particle, and can be measured as twice the angular velocity (ω) of a fluid particle, as shown in equation Equation 2.4 and Equation 2.5 [21].

$$\zeta = \nabla \times \mathbf{V}, \quad (2.4)$$

$$\omega = \frac{\zeta}{2}. \quad (2.5)$$

One way to measure the strength of the rotational field is by circulation (γ), and is given by Equation 2.6 [2].

$$\Gamma = \oint \mathbf{V} \cdot d\mathbf{l} = \int_A \omega d\mathbf{A}, \quad (2.6)$$

where $d\mathbf{l}$ is the vector element of the integration part and $d\mathbf{A}$ is the element of area. The swirl angle, β , shows the intensity of the flow rotation and is defined as

$$\beta = \tan^{-1} \frac{\mathbf{V}_t}{u}, \quad (2.7)$$

where \mathbf{V}_t is the tangential velocity (the velocity in the rotational direction) [22]. A vortex induces a velocity field around the vortex core. If one consider a semi infinite vortex filament with constant circulation, Γ , the induced velocity at a distance, h , perpendicular to the filament can be found by Biot-Savart's law [15],

$$v = \frac{\Gamma}{4\pi h}. \quad (2.8)$$

2.1.3 Wakes

A wake is a region behind a body which is dominated by friction, viscous stress and vorticity, due to separated boundary layers swept downstream by the free stream velocity [21]. When a fluid particle hits the leading edge (LE) of a bluff body, the pressure will rise to the stagnation pressure. The big pressure will force the fluid around the body when a boundary layer, BL, is formed. The BL will separate when Re increases and form a shear layer that will give the wake a boundary. Because of the shear layer, vortices will form, and when these vortices move away from the body and new vortices are created near the cylinder it will form a pattern of vortices migrating downstream. The phenomena is called vortex shedding, and the result is a vortex street [2]. One common vortex street is the Von Karman vortex street as seen in Figure 2.1. Here, vortices that are formed on the upper and lower part of the wake has opposite sign, and the vortices are migrating with a frequency (f). The Strouhal number, St , is the ratio between characteristic flow time and the period of oscillation, and can be calculated using Equation 2.9 [21]. For many shapes, the Strouhal number is available by empirical data.

$$St = \frac{fL_c}{u} \quad (2.9)$$

In a turbulent planar wake, there exists relation for how the lateral length (l) expand and how the difference between the wake velocity and the free stream velocity (U_s) decreases in the streamwise direction (x), shown in Equation 2.11 and Equation 2.10 [20] respectively. This is however only true if the wake has achieved self-similarity, which can only be said to be true for $U_s/U_\infty < 0.1$, i.e the far wake. U_s and l is depicted in Figure 2.2.

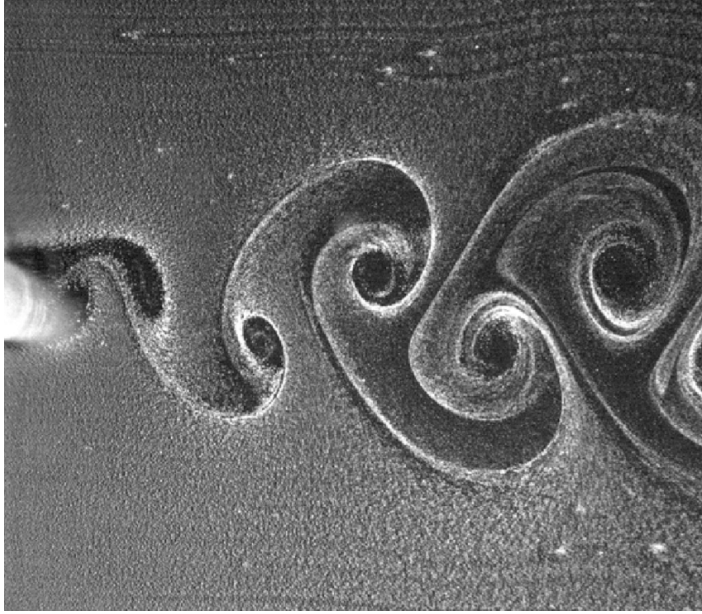


Figure 2.1: A typical Von Karman vortex street [3]

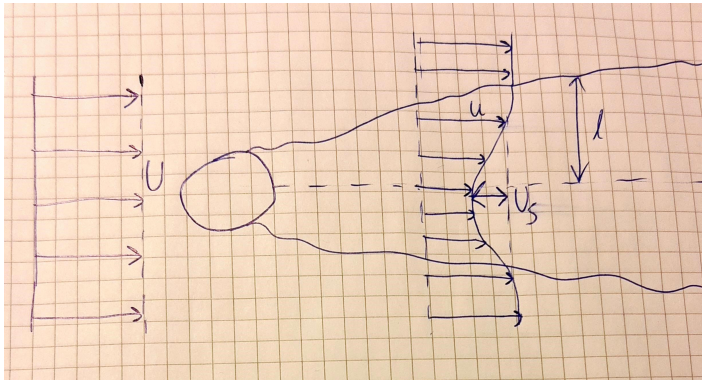


Figure 2.2: Wake

$$U_s \sim x_1^{\frac{1}{2}} \quad (2.10)$$

$$l \sim x_1^{-\frac{1}{2}} \quad (2.11)$$

2.1.4 Lifting line theory

The section lift (F_L') of a finite wing is closely related to circulation. This is evident in the Kutta-Joukowski theorem given in Equation 2.12 [15]

$$F_L' = \rho_\infty u_\infty \Gamma, \quad (2.12)$$

where ρ_∞ is the density of the free stream fluid. Prandtl developed a model for a finite wing, by replacing the wing with a bound vortex filament. As a consequence of Helmholtz vortex theorem, which states that a vortex filament can't end in a fluid, the vortex filament bends at the wing tips and stretch to infinity forming a horseshoe like structure which conveniently depicts the trailing vortices of a wing tip. A single horseshoe structure is not depicting the physics of a real wing because the lift is not evenly distributed over the entire wing. To solve this issue, an infinite amount of horseshoe structures with circulation $d\Gamma_1, d\Gamma_2, d\Gamma_3, \dots$ and spanwise length y_1, y_2, y_3, \dots replace the single horseshoe structure. The structure is shown in Figure 2.3

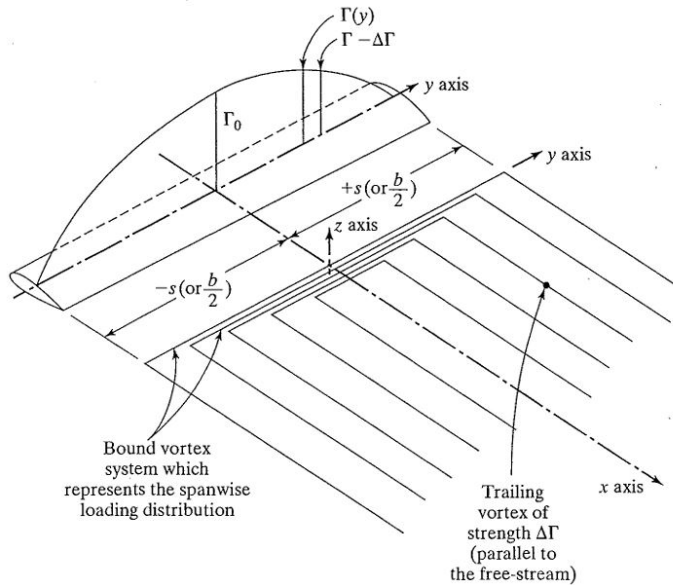


Figure 2.3: Lifting line structure [4]

The distribution of circulation is different for each type of finite wing. The theory

does not take compressibility into account and works best for moderate to high aspect ratios, which is defined as $AR = \frac{b^2}{S}$, where b is the span and S is the area of the wing [20].

2.2 Literature review

The purpose of this literature study is to investigate what type of vortices that can be produced from different shapes and flows. The flow behind a structure exposed to a free stream is often complex and turbulent by nature, which makes an analytical solution to the vortex pattern nearly impossible to find. Therefore, this literature study will be used to find results from previous experiments and Computational Fluid Dynamics (CFD) studies, and look for dependencies between the type of vortex patterns produced as a consequence of the different shapes and flow properties. Relevant parameters for fish migration will also be discussed.

2.2.1 Relevant parameters for fish migration

There are some parameters in a flow that is known to influence the pathway of fish. There are at least two mechanisms that fish can exploit. One of them is to take advantage of the low velocity field in the wake close to an object. The fish can then be called flow refugees. The other mechanism is exploiting the energy of the vortices shedding in a wake, as seen in Figure 2.5. Liao [6] states that this is dependent on the vortex diameter being approximately in the same size ratio as the length of the fish, as well as the flow not having a big background turbulence. For the fish to exploit the energy in the vortices, Cote and Webb [1] suggest comparing the length L , circulation Γ , momentum flux/thrust T and linear impulse I with the relevant fish and vortices. These ratios need to be in a certain value range for the fish to exploit the vortex shedding. The frequency of the vortex shedding may also affect the fish, and it has been shown that rainbow trout synchronize their body motion to the vortex shedding frequency [6]. The parameters and their formulas are summarized in Table 2.1. The literature study will focus on obtaining relations for vortex diameter, circulation, shedding frequency, background turbulence, velocity of wake and maintaining a stable vortex shedding while the density and speed of water is assumed constant. The orientation of the vortices will also be studied. Vortices that induce moments about the fish called yaw, pitch and roll will be studied, see Figure 2.4 for illustration.

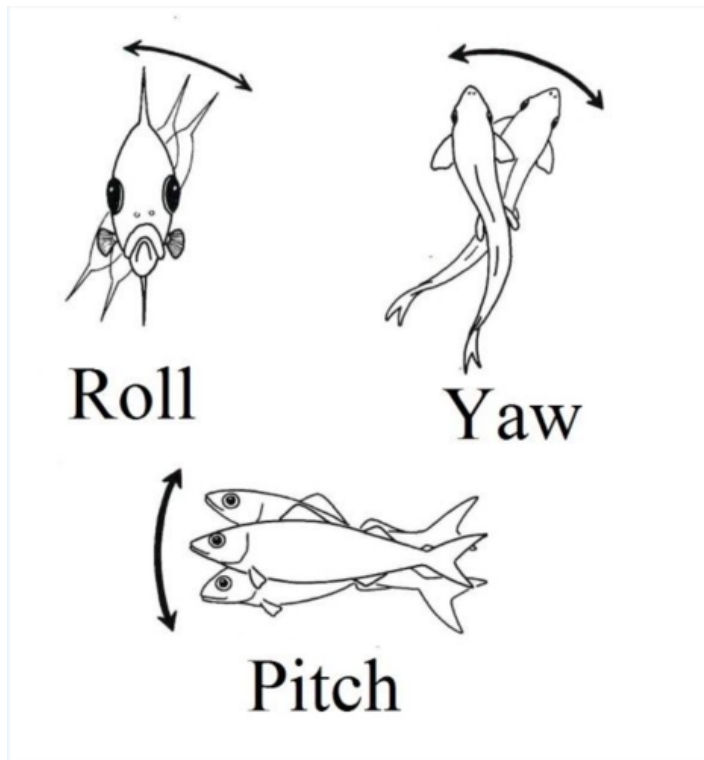


Figure 2.4: Pitch, yaw and roll on a fish [5]



Figure 2.5: A fish exploiting energy in a Von Karman vortex street [6]

Parameter	Eddy	Fish
Length (L)	Eddy diameter	Body length
Circulation (Γ)	$\Gamma_e = \omega_e A_e$	$\Gamma_f = \omega_f A_f = u_f L_f$
Momentum flux / Thrust (T)	$T_e = \rho_e u_e^2 L_e^2$	$T_f = \rho_f u_f^2 L_f^2$
Linear Impulse (I)	$I_e = \rho_e \Gamma_e L_e^2$	$I_f = \rho_f u_f L_e^3$
Frequency (f)	$f_e = \frac{uSt}{L}$	$f_f = \text{frequency of tail beats}$

Table 2.1: Parameters for an eddy and a fish, and how to calculate them. Formulas from [1] and Equation 2.9

2.2.2 Obtaining a Von Karman vortex street behind a circular cylinder

To produce a Von Karman vortex street in the wake of a circular cylinder, a certain range of Reynolds number have to be ensured. If not, the wake can be chaotic and lack a regular shedding frequency. Blevins [2] have made an overview of the results found over several decades by other researchers for the different flow regimes behind a circular cylinder for different Reynolds numbers. The overview is summarized in Table 2.2

It should be noted that a vortex street with a frequency is predictable, and therefore not random. This means that the vortex shedding is laminar, but the flow itself can be turbulent. As the Reynolds number increases, the flow gets increasingly more turbulent. If the freestream velocity is constant, a good measurement of the degree of turbulence is turbulent intensity, as defined in Equation 2.2. There does not exist exact values for how much of TI there will be in a certain wake and exactly how it evolves, but there will be higher TI in the near wake and lower as it evolves in the streamwise direction. A typical evolution in a wake is depicted in Figure 2.6

If the Strouhal number can be found using empirical values of similar cases, the frequency of the shedding can be obtained using Equation 2.9. Figure 2.7 shows Strouhal numbers for different Reynolds number found for a circular cylinder. Another method to modify the frequency is to tilt the cylinder i.e make a yawed cylinder. Chiu and Lienhard [23] shows that the Strouhal number varies with the cosine of the inclination angle up to 60 degrees (see Equation 2.13), and shows that this simple relation correspond well to experimentally found results. Blevins [2] also mention this relation, but suggest using this up to 30 degrees instead of 60, because of increasingly important end effects. Other ways to modify the flow is to vibrate the cylinder perpendicular to the free stream, and Blevins [2] summarize that the vibration near the shedding frequency can among other things strengthen

Table 2.2: Flow regimes behind a circular cylinder [2]

Re	Flow regime
$Re < 5$	The fluid follow the cylinder
$5 < Re < 45$	The boundary layer seperates and creates symmetric vortices close to the cylinder. The longitudinal length of the vortices grows linear with Re, and at $Re = 45$ the length is three times the diameter of the cylinder
$45 < Re < 150$	The wake becomes unstable and one of the vortices breaks away. A laminar vortex street is formed
$150 < Re < 300$	The vortices starts to become turbulent (transition range to turbulence)
$300 < Re < 1.5e5$	The vortex street is fully turbulent and the boundary layer is laminar. The vortex shedding is strong and periodic, and the BL seperates at 80 degrees
$1.5e5 < Re < 3.5e6$	Transitional range. BL becomes turbulent, and seperation at 140 degrees. Laminar seperation bubbles, 3D effects that stops the regular shedding frequency and a big increase in frequency for a smooth cylinder are experienced here
$3.5e6 < Re$	Regular vortex shedding and turbulent BL.

the circulation of the vortices and change the vortex shedding frequency to the cylinder vibration frequency (this is called lock-in). For a regular stationary cylinder, the circulation of shed vortices have been observed to be $1.75 < \Gamma/(uD) < 3.2$, which applies close to the cylinder. The circulation decreases downstream [2].

$$f(\theta) = f(\theta = 0) \cos(\theta), \quad (2.13)$$

where θ is the yaw angle.

As mentioned in subsection 2.1.3 the boundary of the wake is where the seperated boundary layer of the cylinder meets the freestream and forms a shear layer. The size of the wake will therefore start with a lateral length of the diameter of the cylinder, and then grow bigger. The wake is oscillating between vortices formed at lower and the upper part of the cylinder. These vortices use approximately half of the lateral length of the wake, and they have opposite signs as depicted in Figure 2.1. The diameter of the individual vortices will therefore be approximately half of the wake width. In the far wake ($U_s/U_\infty < 0.1$), the lateral half-length, $l_{\frac{1}{2}}$, as well as velocity deficit, U_s is given by asymptotic turbulent wake theory [2] shown

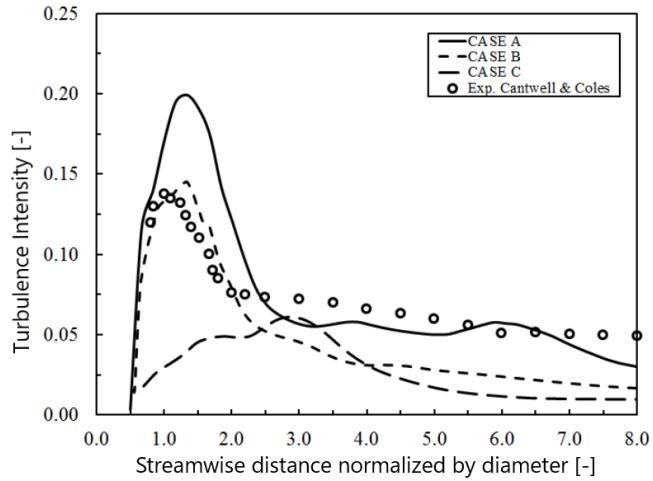


Figure 2.6: Streamwise turbulent intensity [7], where case A, B and C are numerical results. Case A is a smooth cylinder, while case B and C are two versions of grooved cylinders.

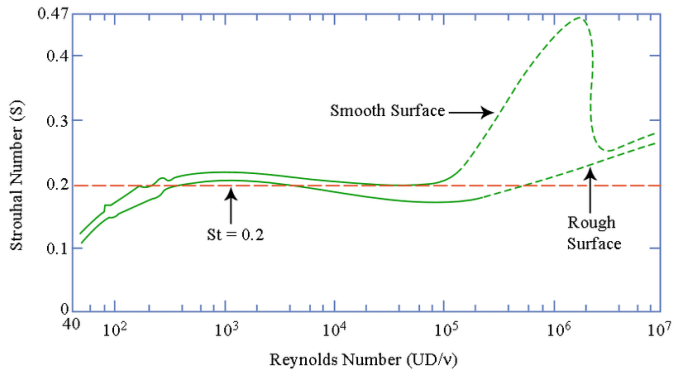


Figure 2.7: St vs Re for a circular cylinder. The figure is plotted by Techet for MIT OSW [8] with data from Lienhard [9], Roshko [10] and Achenbach Heinecke [11]

in subsection 2.1.3. Near the cylinder these relations do not apply, because the flow has not achieved self similarity. There does not exist clear and universal rules in the near wake, but the wake is dominated by vorticity and the non-dimensionalized streamwise velocity has a shape like shown in Figure 2.8. This shape is supported

by other CFD studies and experiments such as Muddada et al [24] and Wissink and Rodi [25]. Interestingly, Figure 2.8 show the wake reach similarity at a shorter distance for bigger Re.

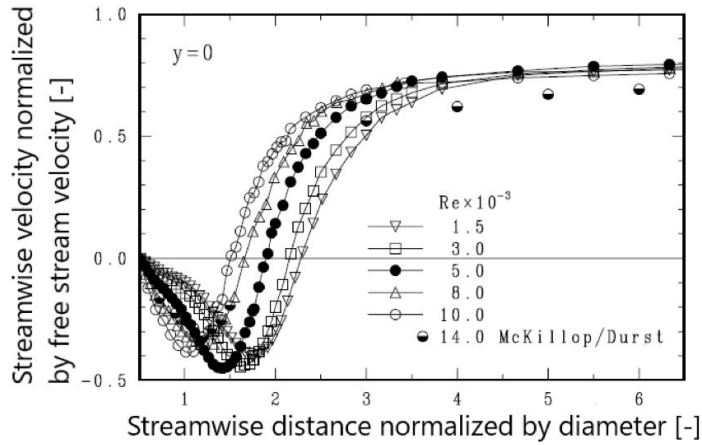


Figure 2.8: Dimensionalized streamwise velocity from experiments behind a circular cylinder [7].

The vortex street described in this subsection can be oriented to make the fish pitch and yaw, but not roll. Making vortices with an orientation to create roll rotation will be discussed in subsection 2.2.4.

2.2.3 Obtaining a Von Karman vortex street behind a non-circular object

Blevins state that "Vortex street wakes tend to be very similar regardless of the geometry of the tripping structure." [2]. In addition, Derakshandeg et al [12] have studied literature on the subject of several non circular shapes and divided the laminar, sub critical, critical and super critical regimes in the same manner as a circular cylinder, which indicates that the overall flow regimes are the same as depicted in Table 2.2. though other parameters vary. Blevins [2] made an overview of how the Strouhal number varies for different Re for a selection of bluff bodies shown in Figure 2.9.

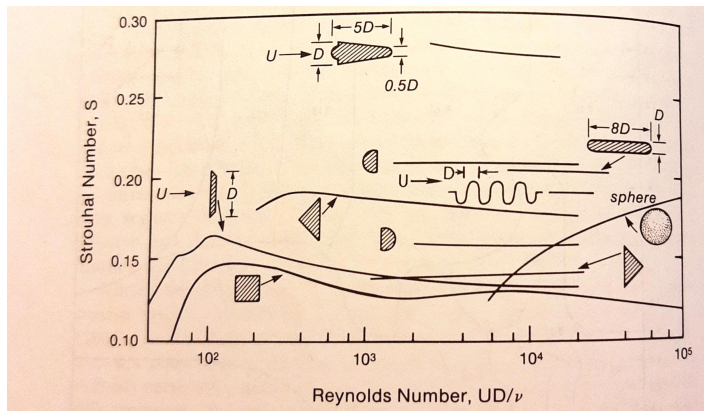


Figure 2.9: Overview of how the Strouhal number varies for different Re for a selection of bluff bodies [2]

One significant difference compared to a circular cylinder is that sharp edged bodies have a fixed separation point independent of Re, while a circular shape changes separation position for different Re. The placement of the separation point alters the wake, and Derakshandeh et al [12] have made an overview of flow regimes for different Re. The focus here, will be on two non-circular objects namely a triangle and square-cylinder, depicted in Figure 2.10

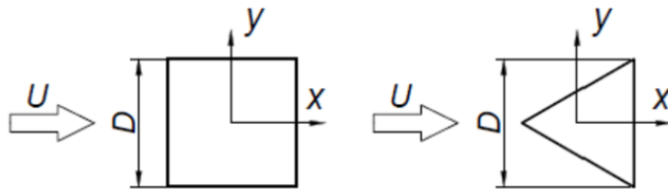


Figure 2.10: The shape of the cross sections that will be studied [12]

Derakshandeh divide the different flow regimes into laminar, subcritical and critical/supercritical. It is worth noting that unlike the circular cylinder, the triangle and square shapes are not as well studied in literature. Therefore, it is difficult to obtain precise relations for circulation, size and overall flow characteristics. Some characteristics for sub critical and critical/super critical are summarized in Table 2.3 and Table 2.4 respectively based on Derakshandeh et al. The laminar flow regime has been left out because the motivation is a flowing river, which will be turbulent.

Parameter	Triangular prism	Square cylinder
Flow description	Seperation at the rear edge	Seperation points are fixed at the edges of the square
Strouhal number	See Figure 2.9	See Figure 2.9
Circulation	Derakshandeh et al. indicate more circulation than a circular and square cylinder.	Can reach 60% more circulation than circular cylinders
Size	Bigger lateral distance between the vortices than for the circular and square cylinder	Smaller lateral distance between the vortices than for the triangular prism

Table 2.3: Wake characteristics of sub critical flow for non circular objects

Parameter	Triangular prism	Square cylinder
Flow description	Re does not influence the wake	Re has a strong influence on the seperated shear layers and therefore the vortex dynamics
Strouhal number	See Figure 2.9	See Figure 2.9
Circulation	–	–
Size of vortices	–	–

Table 2.4: Wake characteristics of critical and super critical flow for non circular objects

The vortex shedding behind non-circular objects like the triangle- and square cylinders can also be oriented to create pitch and yaw moments about the fish, but not roll. Evidence suggest that other shapes that are symmetric in spanwise direction also corresponds well to asymptotic planar wake theory in the far wake [20] as described by Equation 2.10 and Equation 2.11.

2.2.4 Obtaining vortices that creates roll rotation

In the previous two subsections, vortices that can create a yaw and pitch rotation on a fish were discussed. These shapes can not create roll rotation, so a new series of geometries needs to be discussed. The goal is to create vortices with velocity components perpendicular to free stream, and the ability to tune the parameters as well. One example of these type of vortices are trailing vortices at the wing tip of an airplane. As long as the Reynolds number is the same for a wing in water, the vortices should be the same. By using the lifting line theory explained in subsection 2.1.4, the circulation distribution of a wing can be found. At a certain spanwise position the change in circulation equals the circulation of the trailing vortex at that position [15]. This implies that if the lift distribution, and therefore the circulation, is big and evenly distributed with a sudden fall to 0 at the tips, this will result in high concentration of vorticity at the wing tip vortices. If the lift is steadily decreasing to the wing tips the vorticity of the wing tip vortices will be weaker and the circulation more spread out. The shed circulation of a typical large transport aircraft with elliptical lift distribution is depicted in Figure 2.11

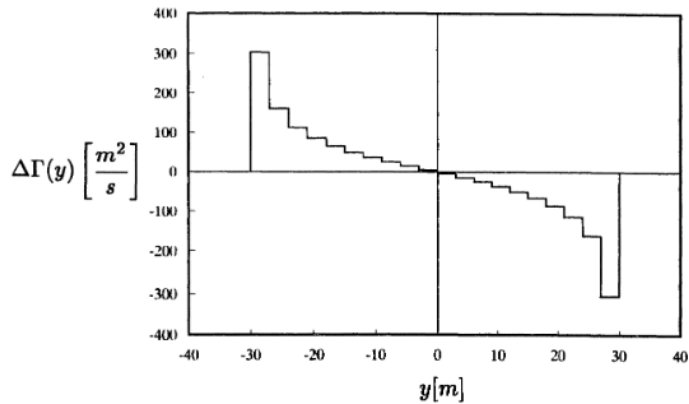


Figure 2.11: Shed circulation of an elliptical loaded wing. $\Gamma_0 = 500m^2/s, b = 60m$ [13]

The tip vortices are apart, but will still influence each other. Using Biot-Savart's law for semi-infinite vortex filaments in Equation 2.8, the induced velocity can be found. Most importantly, the velocity of the wing tip vortices in the downward direction can be found and it is proportional to the circulation and inverse proportional to the wing span. There is no universal definition for vortex size, but something that is often used is looking at the diameter of the core. The core is where the pressure is the lowest, or alternatively where the tangential velocity is the highest. Delisi et

al [26] reports that the velocity cores are in the order of 1 percent of the wingspan. Al-Mahadin and Almajali [27] also states that it's normal to use a relation of vortex cores diameter as a percentage of wing span, but they state that the radius of most of the vortex cores are between 2% and 6%. Both of these investigations suggest that the diameter of the vortices are proportional to the wing span. Delisi et al. also reports that a typical size of smoke trails behind an aircraft is double the size of the cores. Smoke trails might be a good representation of the actual size of a vortex, though there does not exist a clear definition.

Wing tip vortices are known to last for hundreds to thousands of chord lengths downstream [13], making it a persistent vortex regime. Zeman [28] modelled a wing tip vortex, and compared it to experimental data. The results of the study showed that the vortex-core growth rate is controlled by molecular viscosity, and much less of turbulence. The mean vortical flow suppresses the Reynolds shear stress, and the turbulence production rate is nearly zero. This implies that the basic asymptotic planar wake relations discussed in subsection 2.1.3 can not be used to find how long these vortices will last.

For a plane in the air, the lift force usually equals the gravitational force. Therefore, looking at Equation 2.12, the circulation is inversely proportional to the velocity and proportional to the gravitational force and therefore mass (because lift is proportional to circulation and the pilot needs to adjust lift to match the gravitational force). For a wing mounted in a running river, the lift force can be more freely chosen. This means that in general; Lift divided by free stream velocity is proportional to circulation.

Another method to create vortices with velocity components perpendicular to the freestream is by vortex generators. One of them is the half delta wing generator, as seen in Figure 2.12. Vortex generators are well studied in literature, but its focus is on structures smaller than the boundary layer, and its use is transferring more momentum to the boundary layer so that it does not separate as easily. The literature therefore lacks information about the structure of the vortices. The half delta wing has the same physics as a delta wing, but unlike the vortex generator, the vortices created on a delta wing are well covered in literature. Vortices on the delta wing will therefore be the focus in this review.

The primary vortices seen on a delta wing as seen in Figure 2.13, are formed because of boundary layer separation due to a sharp leading edge on a delta wing. The sharp leading edge is bad for the lift to drag ratio, but is needed in supersonic flight, which delta wings are designed for. The pressure gradient between the suction and pressure side in the separated area curls the flow into a primary vortex. This vortex will trail downstream and at a certain location experience a vortex

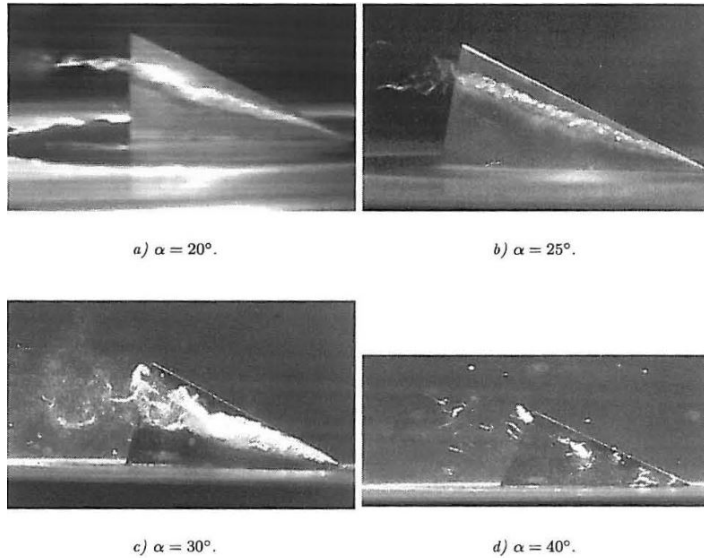


Figure 2.12: Half delta wing vortex generator [14]

breakdown, where the well defined trailing vortex will transition to turbulence [15]. There also exists a secondary smaller vortex beside the primary, which complicates the wake of the delta wing even more.

Precise definitions of vortex life span, circulation, size and turbulence intensity for a certain delta wing are not available, because of its complexity and there are many factors contributing to the resulting flow, but there are some known tuning parameters. From experiments with rounded leading edges, vortices were not formed before the angle of attack (the angle between the freestream and the chordline) were 5° , but for sharp leading edges the vortices appeared at smaller angle of attack. The size of the primary vortex is of the order of half of the wing span [29]. High sweep angles (see Figure 2.14) positions the vortex breakdown further downstream, but the primary vortices will be closer together, and therefore make the vortices asymmetric or unsteady [30]. Direct measurements of a 60° and 70° sweep shows a non-linear growth of the circulation by increasing angle of attack when the breakdown occur downstream, and then shows a more linear growth when the breakdown occurs between the trailing edge and the apex of the wing [31]. The wake after the vortex breakdown downstream is not well covered in literature, and it is complex and sensitive to instabilities. Moreira and Williamson proved in experiments that the wake could persist as long as 650 vortex spans downstream.

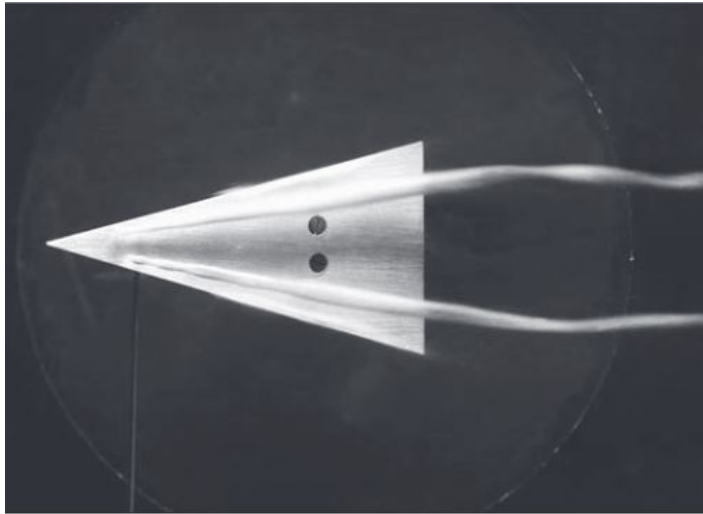


Figure 2.13: Trailing vortices of a delta wing [15]

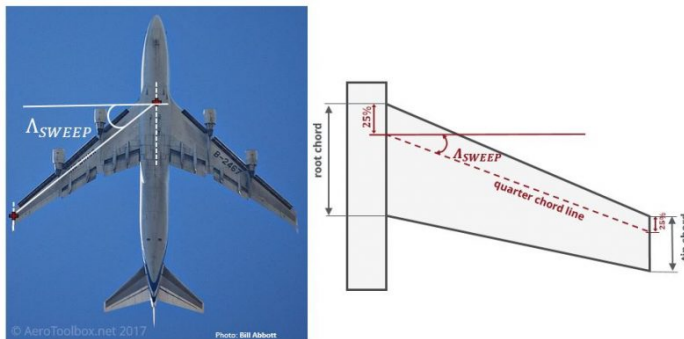


Figure 2.14: The sweep angle [16]. Photo to the left by Bill Abbott

The placement and mechanism of the vortex breakdown is a highly debated subject. Jobe [32] compared 38 data sets from various 65° delta wings with four different empirical vortex breakdown locations prediction methods, but the experiments and methods did not match satisfactory. This illustrates the complex and unpredictable nature of the vortices. Lambourne and Bryer [33] found no clear relations of changing the Reynolds number either. Hall [34] states that for a vortex breakdown to occur, the swirl angle needs to be over 40° . Oledal [14] has written a small sum-

mary mentioning several theories behind the mechanism of the vortex breakdown, but none are fully verified. He also mentions that there exists different types of breakdowns, namely bubble-type, spiral type and double helix breakdown. The reader should address Oledal's review for more information of the different types of breakdowns. One thing that is known, is that increasing the angle of attack will move the placement of the vortex breakdown upstream and will at a critical angle of attack reach the wing and start decreasing the lift. The angle of attack dependency of the placement was also tested experimentally, a typical result is depicted in Figure 2.12.

Chapter 3

Preperation for experiment

Next year, experiments at the Waterpower Laboratory (VKL) will be conducted on several objects in a water channel at NTNU. The cross section of the water channel at VKL is 1m x 1m, and have a maximum volumetric velocity of $0.1m^3s^{-1}$. For the section where the experiments will be held, a rig will be made, see Figure 3.1. This rig will be installed because a test section with good flow quality with arrangements for high quality measurements will be constructed on the rig. The test rig will consist of a converging section, a test section and a diverging section. This chapter will cover theory for designing test rigs and how to measure the flow, and then describe how this particular channel will be designed.

3.1 Previous works - experimental procedure

3.1.1 Particle Image Velocimetry

When performing an experiment with fluid flow, it is desirable to analyze it and examine the velocity field on a digital platform with mathematical values, rather than with film or watching it in real time. One way to do it, is measuring the pressure and temperature and then use physical equations. This can be difficult to do when the fluid or the flow is complex. The measurement devices can also change the nature of the flow [17].

Particle Image Velocimetry (PIV) is a technique that produces local velocity vectors by measuring displacement of particles following the flow in a short time interval. The experimental arrangement of a PIV system is depicted in Figure 3.2, where a camera takes pictures of the Field of Interest (FOV), and a laser illuminate the area with a light sheet. To obtain a light sheet on the desired 2D area, a mirror can be placed with an angle which reflects the light to the area of interest, and lenses can create the desired light sheet size.

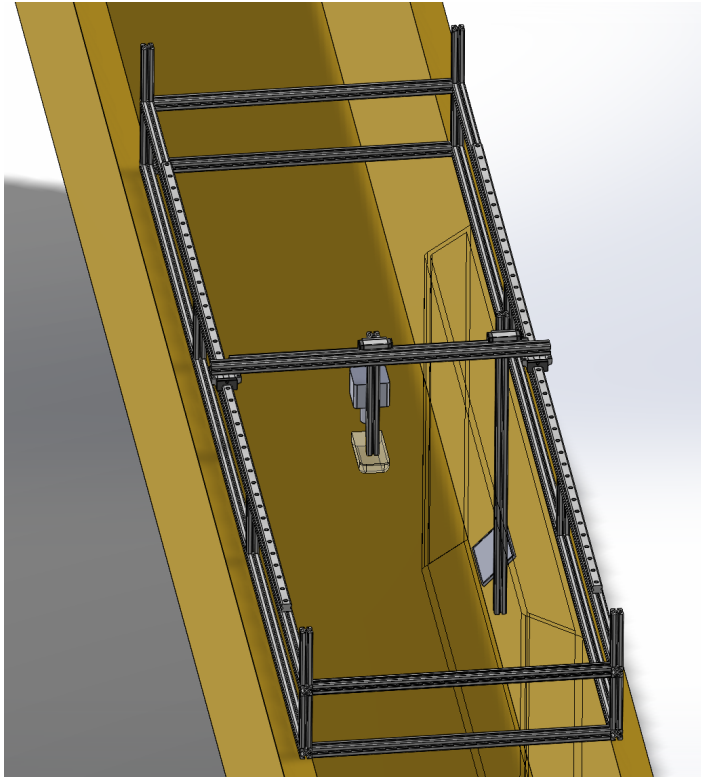


Figure 3.1: Experimental rig in the water channel. Drawing by Bjørn Winther Solemslie.

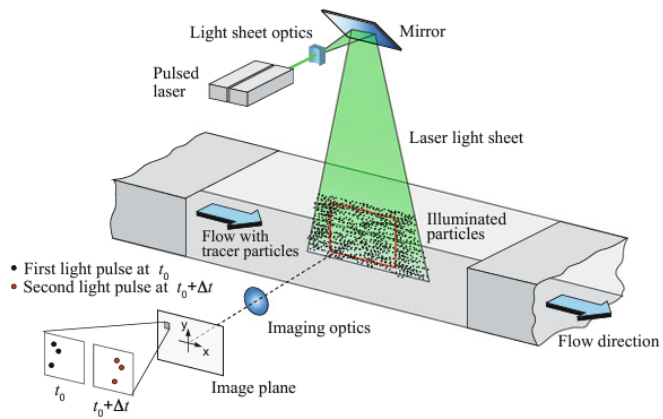


Figure 3.2: Illustration of a PIV set-up [17]

The camera can capture light at a certain angle, which is determined by the sensor size and lens. As seen in Figure 3.3 the angle is decided by the relation between the focal length (length of lens) and the sensor size. The field of view that the camera captures is decided by this angle and the working distance (length between camera and field of view). If a mirror is included in the system, it is important to know that the incidence angle equals the reflection angle [35], as seen in Figure 3.4.

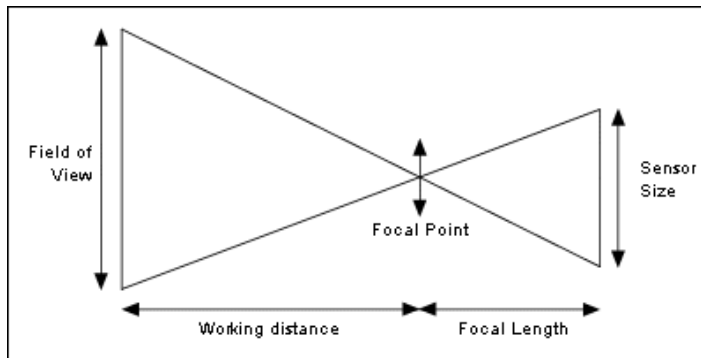


Figure 3.3: Relations between focal length, working distance and field of view [18]

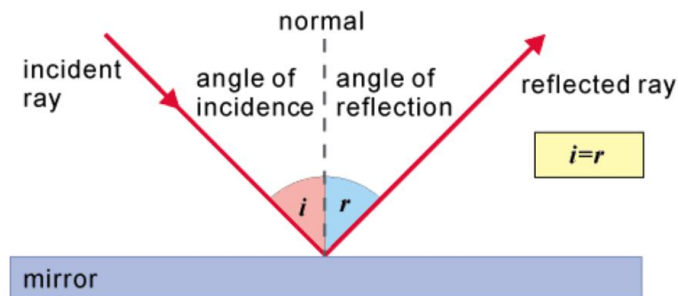


Figure 3.4: The angle of incidence equals the angle of reflection [19]

3.1.2 Design of a test rig in a water channel

There are several considerations to address when designing a test rig in a water channel. In many ways, a low speed wind tunnel has many of the same type of design criteria as for a water channel [36], which is convenient because there exists

more literature on this subject. In fact, many articles on water channel laboratory designs are referring to sources from low speed wing tunnel design, see e.g [37] and [38].

A water channel test rig should have as big contraction ratio (C) as possible [36]. Hernandez et al [39] suggest a contraction ratio between 4.0 – 6.0. This will decrease the turbulence that has evolved either from turns or boundary layer growth in the channel before the test section, and make the flow more uniform. Another way to decrease the turbulence is by honeycomb or screens, which are structures with grids. One typical contraction curve for water channels is the Witozinsky curve, given in Equation 3.1 [40]. The length of the contraction is important. A long length will grow a bigger boundary layer which will make the flow less uniform, while a short length may create local regions of adverse pressure gradient which seperates the flow. Hernàndez et al suggest an angle in the order of 12° between the inlet and outlet of the converging section [39].

$$\left(\frac{l_{\frac{1}{2}}}{y}\right)^2 = 1 - \left(1 - \frac{1}{C^2} \frac{[1 - (\frac{x}{L_{conv}})^2]^2}{[1 + \frac{1}{3}(\frac{x}{L_{conv}})^2]^3}\right)^2, \quad (3.1)$$

where $l_{\frac{1}{2}}$ is half of the converging outlet height and L_{conv} is the length of the converging section.

The blockage ratio is defined as frontal area of the object at interest and the cross sectional area of the testing section, and this should not exceed 7.5%. If it does, the channel wall will affect the flow adversely, and not depict a real non-obstructed flow. One key difference between a channel and a tunnel is the free surface, and if the experiments do not want the effect of the surface waves, the objects should be fully submerged in the water and the Froude number, Fr , defined in Equation 3.2, should be lower than 1, preferably by an order of magnitude [21].

$$Fr = \frac{u}{\sqrt{gd}}, \quad (3.2)$$

where d is the depth of the water. The test section length should be somewhere between 0.5-3 times the hydraulic diameter to get a uniform flow, while avoid seperation at the diverging section. A good trade off is a length of 2 times the hydraulic diameter [41]. The hydraulic diameter is defined in Equation 3.3 [21].

$$D_h = \frac{4A}{P}, \quad (3.3)$$

where P is the wetted perimeter. The diverging section must prevent seperation,

but also prevent stall. Hernandez et al [39] says the diverging angle must not be smaller than 3.5° . Another design aspect is to ensure that the object in the test section is hydraulically smooth. This means that the flow should not be affected by roughness (ϵ) from the object. White [42] has set a criteria for a object to be hydraulically smooth, which is

$$u^* < \frac{5\nu}{\epsilon}, \quad (3.4)$$

where u^* is the friction velocity and can be found using

$$u^* = \sqrt{\frac{\tau_w}{\rho}}, \quad (3.5)$$

where τ_w is the wall shear stress.

3.2 Design and preparations for experiment

With the theory and considerations from section 3.1, a experimental set up is possible to obtain. Figure 3.6 shows the different cases that can be relevant for the PIV system. Because the side walls are non-transparent, a mirror in the space between the contracted test section and the channel needs to be installed. This is because the laser or the camera needs a point of view that is not reachable from the top surface. An example of this is illustrated in Figure 3.5. The field of view is dictated by the sensor size, focal length, the size of the mirror and the angle of the mirror. If the camera can be fitted inside the mirror space, large focal point angles is obtainable because the camera is close to the mirror. This assumes the right type of lens can be arranged. The required size of the cross sectional area is uncertain at this point, because there is not fully planned what types of objects that will be tested for the FishPath project yet. Preferably, there are some slack on the size of the area to account for changes to come.

The considerations that is needed to design the contraction, test section and diffusor is summarized in Table 3.1, and is based on section 3.1. There are some constraints that requires the opposite design e.g wanting a high contraction rate, but a blockage factor of less than 7.5%. Some details of the constraints are not yet decided. Many PIV considerations are not analysed in this project, and will need to be done before the upcoming experiments. Examples of this is size and type of particles in the flow (seeding), type of camera and laser lenses, and the maximum and minimum size of the FOV for detailed velocity fields of complex flows. A suggestion for the resulting design based on Table 3.1 can be seen in the Result, section 4.2, but keep in mind that this is not the final design, since some parameters will need some clarifications.

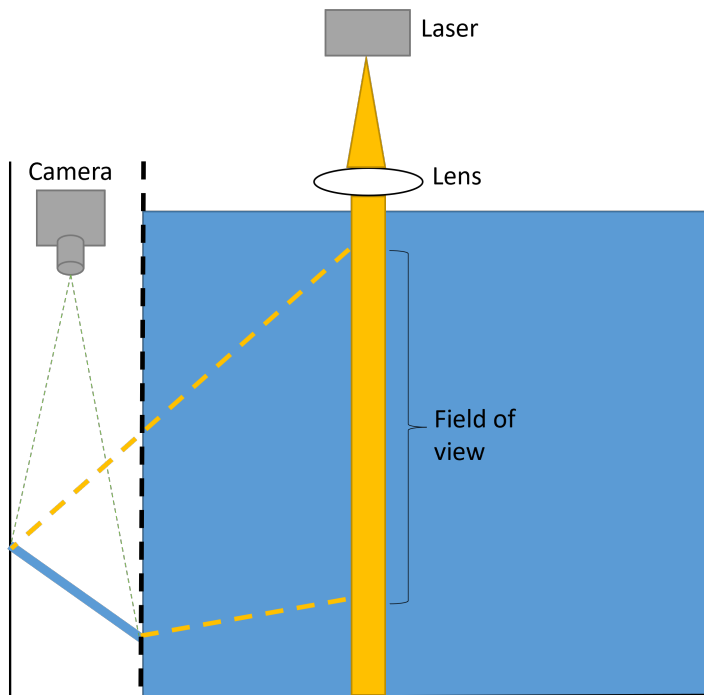


Figure 3.5: The concept of performing PIV in a non-transparent water channel.

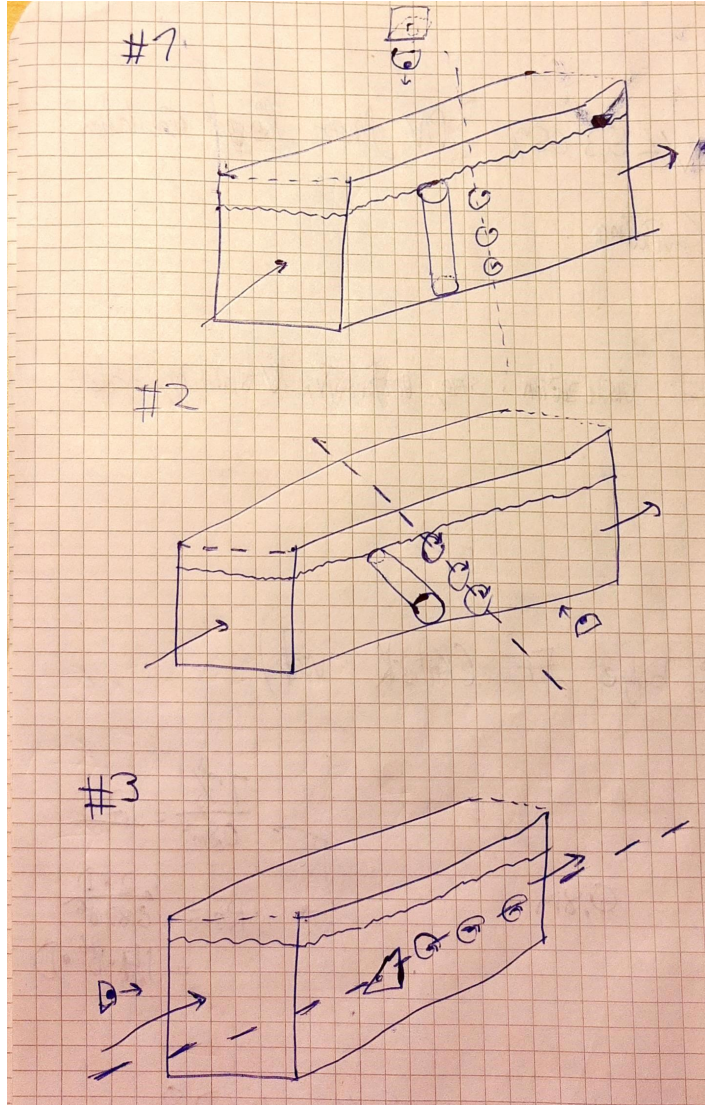


Figure 3.6: Flows that will be considered captured by PIV. The side walls are solids that can not be seen through.

Table 3.1: Design consideration for designing the experimental rig at VKL.

Design consideration	Constraint
Contraction ratio	As big as possible, preferably between 4.0 to 6.0. Can possibly be reduced with flow straighteners
Contraction curvature	Witozinsky curve
Contraction length	Angle between inlet and outlet of contraction should be in the order of 12°
Blockage	The frontal area of object to cross section area should be less than 7.5%
Test section length	Should be 2 times the hydraulic diameter
Diverging ratio	Same as contraction ratio
Diffusor curvature	Linear
Diffusor length	The diverging angle must not be smaller than 3.5°
Reynolds number range	The Reynold number range needed for the experiments is uncertain at this point
Froude number	Should be less lower than 1, preferably 0.1.
Size of FOV	Not certain at this point
Hydraulically smooth	The roughness from the 3D printer is unknown at this moment
Blockage	The frontal area of object to cross section area should be less than 7.5%
Place for mirror	Enough space for the camera at VKL.
Cross sectional area	As big as possible.
Volumetric velocity	Maximum $0.1m^3s^{-1}$

Chapter 4

Results and discussions

4.1 Vortex tuning

Table 4.1: Vortex tuning for a delta half wing vortex generator

Vortex variable	Methods for tuning
Stable flow regime	Avoid vortex breakdown on the wing by having a moderate angle of attack and having a big enough sweep angle. Avoid very large sweep angles because this creates asymmetrical or unsteady vortices.
Size	Size of the primary vortices are of half the order of the wing span.
Circulation	There is a unlinear growth of circulation by increasing the angle of attack until the point where the breakdown occurs on the wing. From there, a more linear growth of circulation occurs where the breakdown is between the trailing edge and the apex of the wing.
Velocity and life span	After the breakdown, a turbulent wake is formed. It can persist as long as 650 vortex spans downstream.
Orientation	Roll.

Table 4.2: Vortex tuning for a Von Karman street

Vortex variable	Methods for tuning
Stable flow regime	Regular vortex shedding for a circular cylinder: $300 < Re < 1.5e5$ and $3.5e6 < Re$. Derakhshandeh and Alam [12] keeps the limits for cylinders with triangular and square cross-sections the same
Size	The lateral size of the wake behind objects is the same as the object. It will then grow which can not be perfectly quantified until $U_s/U_\infty < 0.1$. Then $l \sim x_1^{-\frac{1}{2}}$. The vortex diameter is approximately half of the wake lateral size.
Circulation	Close to a circular cylinder, $1.75 < \Gamma/(uD) < 3.2$, and then the circulation decreases downstream. This makes the diameter a variable to modify to change the circulation. A square cylinder have been found to increase circulation to 60% compared to a circular cylinder, a triangular even more. Vibrating the cylinder can also increase the circulation.
Frequency	Use empirical values for the Strouhal number for the shape and flow condition of interest, and modify the frequency by changing shape or characteristic length. Another tuning option is yawing the cylinder using $f(\theta) = f(\theta = 0) \cos(\theta)$.
Velocity and lifespan	The streamwise velocity will decrease fast in the near wake, and then follow planar asymptotic wake theory in the far wake. The vortices will loose its circulation in the streamwise direction.
Orientation	Pitch and yaw.

Table 4.3: Vortex tuning for a wing tip

Vortex variable	Methods for tuning
Stable flow regime	Using a wing with an even lift distribution, e.g a rectangular wing, will create vortices that are smaller but more concentrated. If a wing has a lift distribution that constantly decreases from the root, the vortices will be bigger, but more weak and diffused.
Size	Radius of vortex cores are reported to be between 1% – 6% of the wing span. Visual inspections indicate that smoke trails from airplanes is double the size of vortex cores. Smoke trails could be a more relevant size measurement of vortex diameter.
Circulation	Obtain the spanwise circulation distribution for lifting line theory. At a certain spanwise position, the change in spanwise circulation equals the circulation of the trailing vortex. This means picking a wing that has a sudden decrease in circulation/lift will result in a stronger circulation. To obtain a bigger drop, a bigger lift can be ensured with aircraft modifications such as changing the angle of attack or switching the type of airfoil used.
Velocity and life span	The vortices and the streamwise velocity in the wake do not influence each other in a substantial way. The vortices has been observed to remain for hundreds to thousands of chord lengths downstream
Orientation	Roll.

Table 4.1, Table 4.2 and Table 4.3 summarize how to tune vortex parameters for half delta wing vortex generators, Von Karman vortex streets and wing tips respectively. The tables are a result of the literature review from section 2.2. Looking at these tables, there is a varying degree of how precise the discription of the vortex parameters are and how they change. There exists other fluid dynamic problems where good empirical methods have been established, e.g pipe flow. By using Moody diagram and knowing the Reynolds number and surface roughness, one can calculate the pressure loss which can be used to measure the pump capacity needed to move the fluid through the pipe. There does not exist such simple relations for vortices behind objects today, though some cases are better covered in literature than others. The cylinder case is well studied, and is the case where the most specific

results and methods for tuning parameters were found in this study. On the other hand, vortex generator literature lacks a detailed description of the vortices themselves. There exists literature to a great extent on lift, drag and stall of wings, but less reviews on the circulation and size of the trailing vortices. This is the reason why the wing tip and delta wing generator vortices have relations between parameters rather than precise values. For example, the vortex breakdown placement of a delta wing can not be precisely calculated, but the placement can move downstream if the angle of attack is increased.

Many of the vortex tuning methods for each parameter are affecting other parameters. An example is decreasing the vortex size in a Von Karman street. A simple way to do that is decreasing the diameter of the object. By doing so, the frequency will also be changed. This can be fixed in the cases where a vortex parameter can be tuned by several methods. In the cylinder case, you can adjust the frequency by yawing the cylinder to remedy for the decrease in diameter. In some cases this is not possible, so then a trade-off must be made.

In this literature review, many of the findings is related to airflow. The motivation for this project is water, so it is important to ensure that same relations apply. The Reynolds number needs to be same for both cases to ensure similar flow behaviour, and the good thing about water is that the kinematic viscosity is lower, which facilitates watching the same air flow phenomena at lower velocity. Air can be compressed and water is assumed an incompressible fluid. However, air is assumed incompressible for the low wind speeds assessed in this literature review. Another aspects worth mentioning is that water can experience cavitation, which is evaporated water bubbles formed because of low pressure. This is also assumed not relevant for this project, due to the relatively low velocities in a river. Finally, water in an open channel can experience waves or critical flow. This can affect the result, and the Froude number must be carefully assessed.

One thing that recurs is the lack of detailed description of the near wake, the turbulence intensity and the evolution of circulation downstream. It looks like these parameters are difficult to generalize, and depends on case to case. Hopefully, this will improve with more studies in the future. This is important for the motivation of this project, because the turbulence intensity and how the wake evolves downstream can be important parameters for influencing fish migration.

4.2 Experimental test section

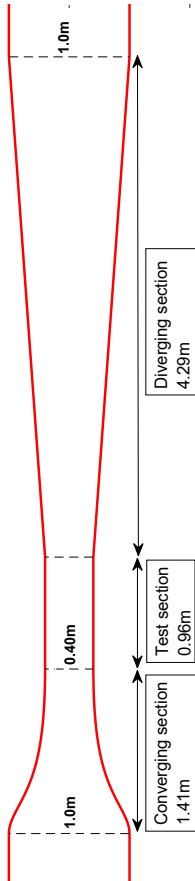


Figure 4.1: Design proposal for the water channel, birds eye view.

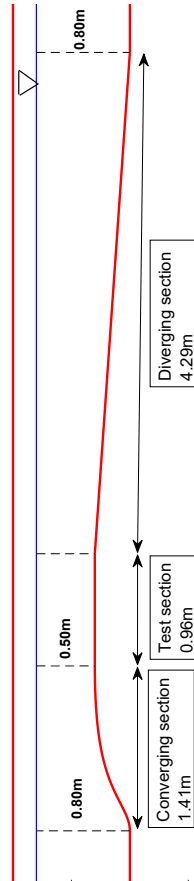


Figure 4.2: Design proposal for the water channel, sideways view

Table 4.4: Experimental rig parameters for the suggested design.

Experimental rig parameter	Value
Contraction ratio	4.0
Diverging angle	4°
Water height in test section	0.5m
Water width in test section	0.4m
Cross sectional area in test section	0.2m ²
Length of test section	0.96m
Total length	6.7m
Froude number	0.23 at most
Width for mirror and wall	0.3m

Figure 4.1 and Figure 4.2 show a suggestion for the design of the experimental set up. Table 4.4 shows key parameters for this design. A contraction ratio of 4, 30cm width for the mirror and a small Froude small number are good results based on the constraints from section 3.2. When the plans for the experiment are settled, the objects must fulfill the remaining constraints. To ensure a blockage ratio of less than 7.5% the maximum projected area allowed will be 150cm². The object must be hydraulically smooth, and the Reynolds number of interest must be obtained.

Flow straighteners will be added before the test section to further uniformize the flow. For this design, the contraction is performed in the same way for both the side walls and the bottom of the channel. There may be a better way to do this, but no literature was found on the subject.

Chapter 5

Conclusions

The purpose of this paper was to find relevant literature to facilitate the generation of different types of vortices and wakes, and modify the properties that are relevant for fish migration. More specifically the ability to obtain a stable flow regime and predict the circulation, shedding frequency, size, orientation, streamwise velocity and temporal stability of the vortices has been the main focus. These findings will be validated in experiments later, hence a test rig design proposal has been created.

The wake behind cylinders with circular, triangular and square cross sections as well as the half delta wing vortex generator and wing tips, were investigated. The results show a wide range of precision. The vast amount of empirical data for the circular cylinder provides precise predictions for how to modify vortex properties, whereas the triangular and square cylinders have less studies resulting in less accurate predictions. The delta wing and the wing tip has been well studied for their performance in aerodynamic flight, but the vortices themselves are not equally well covered. Here, there exist good relations between parameters, but it does not provide prediction with exact values.

The result of the literature review will be tested experimentally, and a design for the experimental rig has been proposed to ensure good flow qualities and the ability to do a PIV measurement in the water flume at the Waterpower Laboratory. If good methods for modifying vortex parameters are identified, the experiments on real fish will be able to isolate what type of vortex modifications that influence the path of a fish migrating downstream rivers. This could be the low-cost and reliable approach for preventing fish from entering waterpower plant intakes in the future.

Chapter 6

Future work

The results from the literature in this paper need to be verified with experiments. More studies for different flows on wakes behind cylinders with non-circular cross sections will make vortex tuning studies in the future easier and increase the precision. This is also true for the vortices themselves behind half delta vortex generators and wing tips. Vortex generator studies today are mostly focused on structures with sizes below the boundary layer, because its use is to keep boundary layers attached longer. Therefore, more studies on large scale vortex generators would be helpful. The size of vortices are not strictly defined today. When comparing the size of a fish to the size of a vortex, there is no definition of the vortex size. There exists vortex core definitions, but the vortex is still influential on the area beyond this point, so this is an important definition that needs to be set for further studies. A vortex parameter that has not been addressed in this thesis is the angle of the vortices trailing downstream with respect to the streamwise velocity. This as well as the study of several objects in a grid could be a influential parameter for the FishPath project.

References

- [1] Cote, A. J. and Webb, P. W., 2015, "Living in a turbulent world - A new conceptual framework for the interactions of fish and eddies," *Integrative and Comparative Biology* (Vol. 55), Oxford University Press.
- [2] Blevins, R. D., 1994, *Flow-Induced Vibration*, Krieger.
- [3] Huang, L., Daniela Benites, Lyu, S., Smith, T., Li, M., Shang, Y., and Klettner, C., 2019, "UCL OpenFOAM Course 2019," .
- [4] Bertin, J. J. and Cummings, R. M., 2008, "Aerodynamics for engineers," .
- [5] Mackean, D. G., *Fish Fins. Roll & Yaw & Pitch*, <http://www.biology-resources.com/drawing-fish-pitch-roll-yaw.html>, Date accessed: 12.12.2021.
- [6] Liao, J. C., 2007, "A review of fish swimming mechanics and behaviour in altered flows," .
- [7] Norberg, C., 1998, "LDV-measurements in the near wake of a circular cylinder," .
- [8] Techet, A. H., 2005, *13.42 Lecture: Vortex Induced Vibrations*, Massachusetts Institute of Technology, Open Courseware.
- [9] Lienhard, J. H., 1966, "Synopsis of lift, drag and vortex frequency data for rigid circular cylinders," .
- [10] Roshko, A., 1955, "On the Wake and Drag of Bluff Bodies," .
- [11] Achenbach, E. and Heinecke, E., 1981, "On vortex shedding from smooth and rough cylinders in the range of Reynolds numbers 6×10^3 to 5×10^6 ," .

- [12] Derakhshandeh, J. F. and Alam, M. M., 2019, "A review of bluff body wakes," .
- [13] Green, S. I., 1995, *FLUID VORTICES*, Springer-Science+Business Media.
- [14] Oledal, M., 2001, "Cavitation in Complex Separated Flows," .
- [15] Anderson, J. D., 2017, *Fundamentals of Aerodynamics*, McGraw-Hill.
- [16] AeroToolbox, 2017, *Sweep angle and supersonic flight*, AeroToolbox.com/intro-sweep-angle/, date accessed: 16.12.2021.
- [17] Raffel, M., Willert, C. E., Scarano, F., Kähler, C. J., Wereley, S. T., and Kompenhans, J., 2018, *Particle Image Velocimetry A Practical Guide*, Springer International Publishing.
- [18] Channel Systems Inc., *Field of View & Focal Length Diagram*, <https://www.channelsystems.ca/calculators/field-of-view>, date accessed: 12.12.2021.
- [19] Edexcel Physics IGCSE, 2016, "3.15 use the law of reflection," <https://physicsigcse.wordpress.com/2016/05/06/3-15-use-the-law-of-reflection-the-angle-of-incidence-equals-the-angle-of-reflection/>, Date accessed: 16.12.2021.
- [20] Pope, S. B., 2000, *Turbulent Flows*, 1st ed., Cambridge University Press.
- [21] Cengel, Y. A. and Cimbala, J. M., 2014, *Fluid Mechanics*, McGraw-Hill.
- [22] Kim, C. G., Kim, B. H., Bang, B. H., and Lee, Y. H., 2015, "Experimental and CFD analysis for prediction of vortex and swirl angle in the pump sump station model," *IOP Conference Series: Materials Science and Engineering* (Vol. 72), Institute of Physics Publishing.
- [23] Chiu, W. S. and Lienhard, J. H., 1967, "On Real Fluid Flow Over Yawed Circular Cylinders," .
- [24] Muddada, S., Hariharan, K., Sanapala, V., and Patnaik, B., 2021, "Circular cylinder wakes and their control under the influence of oscillatory flows: A numerical study," .
- [25] Wissink, J. G. and Rodi, W., 2008, "Numerical study of the near wake of a circular cylinder," .

-
- [26] Delisi, D. P., Greene, G. C., Robins, R. E., Vicroy, D. C., and Wang, F. Y., 2003, "Aircraft wake vortex core size measurements," *21st AIAA Applied Aerodynamics Conference*, American Institute of Aeronautics and Astronautics Inc.
- [27] Al-Mahadin, A. and Almajali, M., "Simplified Mathematical Modelling of Wing Tip Vortices," .
- [28] Zeman, O., 1995, "The persistence of trailing vortices: A modeling study," .
- [29] Brebbia, C. A. and Orszag, S. A., 1989, "Lecture Notes in Engineering," .
- [30] Miller, G. D. and Williamson, C. H. K., 1997, "Turbulent Structures in the Trailing Vortex Wake of a Delta Wing," .
- [31] Moreira, J. and Johari, H., 1997, "Direct measurement of delta wing vortex circulation using ultrasound," *35th Aerospace Sciences Meeting and Exhibit*, American Institute of Aeronautics and Astronautics Inc, AIAA.
- [32] Jobe, C. E., 2004, "Vortex breakdown location over 65 degrees delta wings empiricism and experiment," .
- [33] Lambourne, N. C. and Bryer, D. W., 1962, "The Bursting of Leading-Edge Vortices Some Observations and Discussion of the Phenomenon," .
- [34] Hall, M. G., 1972, "VORTEX BREAKDOWN," .
- [35] Crowell, B., 2006, *Discover Physics*, Light and Matter.
- [36] Zhang, H., 2017, "The Water Tunnel/Channel Design and Application in Beihang University," .
- [37] Roque, G., Ássi, S., Meneghini, J. R., Augusto, J., Aranha, P., George, W., and Coletto, P., 2005, "DESIGN, ASSEMBLING AND VERIFICATION OF A CIRCULATING WATER CHANNEL FACILITY FOR FLUID DYNAMICS EXPERIMENTS," .
- [38] Eslam Panah, A. and Barakati, A., 2017, "Design and Build a Water Channel for a Fluid Dynamics Lab," .
- [39] Hernández, M. A. G., López, A. I. M., Jarzabek, A. A., Perales, J. M., Wu, Y., and Xiaoxiao, S., 2013, "Design Methodology for a Quick and Low-Cost Wind tunnel," .
- [40] Yin, F., Xue, L., Liu, Z., Li, L., and Wang, C., 2019, "Structure optimization of separating nozzle for waste plastic recycling," *Procedia CIRP* (Vol. 80), Elsevier B.V.

- [41] Mauro S, Brusca S, Lanzafame R, Famoso F, Galvagno A, and Messina M, 2017, “Small-Scale Open-Circuit Wind Tunnel: Design Criteria, Construction and Calibration,” .
- [42] White, F. M., 2011, *Fluid Mechanics*, McGraw-Hill.

Appendices

Appendix A

```
% MATLAB script Design2.m
% Design of a water channel section
% By Simon Urdahl 15.12.2021

clc
clear all
close all

%% Defining parameters

C = 4; % Contraction ratio
depth = 0.8; % Depth of water

h = depth-0.5;
r = roots([1 h -0.5*depth/C]);
r_star = max(r); %Half-length of contracted area
C_width = 0.5/r_star; %Contraction ratio of the bottom part
% of channel

w = 2*r_star; %Width in channel
mirror = (1-2*r_star)/2; %Width for the mirror space
L_c = (mirror)/tan(deg2rad(12)); %Length of contraction
area = w*(depth-r_star); %Cross sectional area
perimeter = 2*depth + w; %Wetted perimeter
D_h = 4*area/perimeter; % Hydraulic diameter
L_test = 2*D_h; %Length of test section
div_angle = 4; %The angle of the diverging section
L_div = (mirror)/tan(deg2rad(div_angle)); %The length of the
```

%diverging section

%% Creating axes

```
x_start = linspace(0,0.5);
x_c = linspace(0.5,0.5+L_c);
x_test = linspace(x_c(end),x_c(end)+L_test);
x_div = linspace(x_test(end),x_test(end)+L_div);
x_end = linspace(x_div(end),x_div(end)+0.5);
```

```
y_start1 = ones(1,length(x_start))*0.5;
y_c1 = (r_star)./sqrt((1-(1-(1/C_width^2))*(1-((x_c-0.5) ...
/L_c).^2).^2 ./ (1+(1/3)*((x_c-0.5)./L_c).^2).^3));
y_start2 = ones(1,length(x_start))*(-0.5);
y_c2 = 0 - y_c1;
```

```
y_test1 = ones(1,length(x_test))*y_c1(end);
y_test2 = ones(1,length(x_test))*y_c2(end);
```

```
a = (0.5-y_test1(end))/L_div; % Derivative of linear
%diverging section
```

```
y_div1 = (x_div-x_test(end))*a+y_test1(end);
y_div2 = 0-y_div1;
```

```
y_end1 = ones(1,length(x_end))*0.5;
y_end2 = y_end1*(-1);
```

```
x_horizontal = linspace(0,x_end(end));
y_horizontal = ones(1,length(x_horizontal))*0.5;
y_horizontal2 = ones(1,length(x_horizontal))*(depth-0.5);
```

%% Plotting

```
figure(1)
plot(x_start,y_start1,x_start,y_start2,x_c,y_c1,x_c,y_c2,x_test,...
y_test1,x_test,y_test2,x_div,y_div1,x_div,y_div2,x_end,y_end1,...
x_end,y_end2,'Color','r','LineWidth',2)
hold on
```

```
y__test = linspace(y_test2(1),y_test1(1));
x__test = linspace(x_test(1),x_test(1));
plot(x__test,y__test,'--k')
```

```

hold on

y__test = linspace(y_test2(end),y_test1(end));
x__test = linspace(x_test(end),x_test(end));
plot(x__test,y__test,'--k')
hold on

y__c = linspace(y_c2(1),y_c1(1));
x__c = linspace(x_c(1),x_c(1));
plot(x__c,y__c,'--k')
hold on

plot([x_div(end),x_div(end)],[y_div1(end),y_div2(end)'],'--k')
axis equal
title('Water channel design, birds eye view')
xlabel('Length [m]')
ylabel('Width [m]')

%%%%%%%%%%%%%%%%%%%%%%%%%%%%%%%%%%%%%%%%%%%%%%%%%%%%%%%%%%%%%%%%%%%%%%%%
figure(2)
plot(x_horizontal,y_horizontal,x_start,y_start2,x_c,y_c2,...
x_test,y_test2,x_div,y_div2,x_end,y_end2,'Color','r',...
'LineWidth',2)
hold on

plot(x_horizontal,y_horizontal2,'b')
hold on

plot([x_start(end),x_start(end)],[y_start2(end),depth-0.5],'--k')
hold on

plot([x_c(end),x_c(end)],[depth-0.5,y_c2(end)'],'--k')
hold on

plot([x_test(end),x_test(end)],[depth-0.5,y_test2(end)'],'--k')
hold on

plot([x_div(end),x_div(end)],[depth-0.5,y_div2(end)'],'--k')
axis equal
title('Water channel design, side view')
xlabel('Length [m]')

```

```
ylabel('Height [m]')
```

```
%% Results
```

```
fprintf('Area = %f m^2, width = %f m, height = %fm',...)
```

```
(r_star+h)*2*r_star,2*r_star,h+r_star)
```

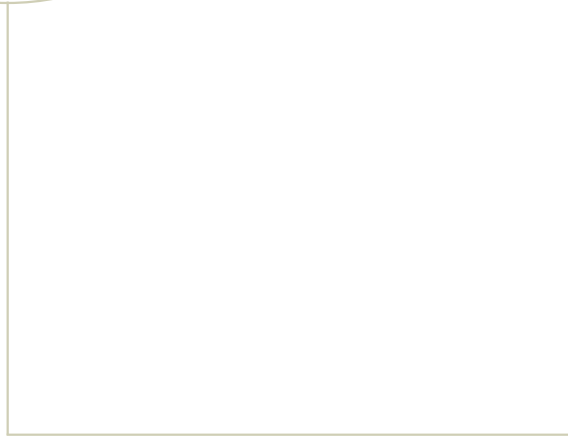
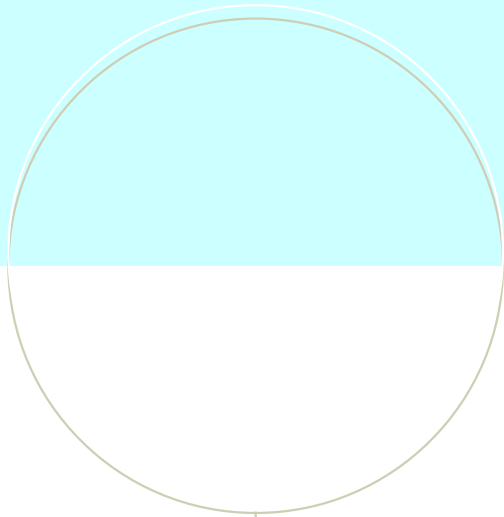
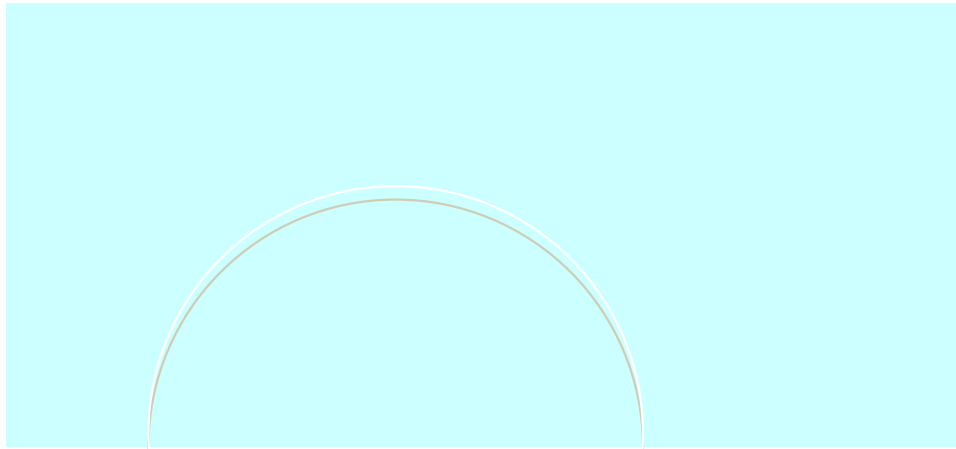
```
fprintf(' and contraction ratio = %f. \n',C)
```

```
fprintf('Length of test section = %fm. Total length is: %fm',...)
```

```
    L_test,L_c+L_test+L_div)
```

```
fprintf('\n If total length is too long, reduce the diverging')
```

```
fprintf(' angle down to minimum 3.5 degrees')
```



NTNU – Trondheim
Norwegian University of
Science and Technology